



# Different Risk Profiles for Progression of Nonproliferative Diabetic Retinopathy: A 2-Year Study

Inês P. Marques · Maria L. Ribeiro · Torcato P. Santos ·  
Luis G. Mendes · Débora Reste-Ferreira · Ana R. Santos ·  
Conceição L. Lobo · José G. Cunha-Vaz

Received: November 4, 2022 / Accepted: November 23, 2022 / Published online: December 10, 2022  
© The Author(s) 2022

## ABSTRACT

**Introduction:** Characterization of 2-year progression of different risk phenotypes in eyes with mild and moderate nonproliferative diabetic retinopathy (NPDR) in type 2 diabetes (T2D).

**Methods:** A 2-year prospective longitudinal cohort study (CORDIS, NCT03696810) was conducted. Ophthalmological examinations were performed including best corrected visual acuity, color fundus photography and optical coherence tomography (OCT and OCTA). OCT metrics, central retinal thickness and ganglion cell layer + inner plexiform layer (GCL + IPL)

thickness were analyzed. OCTA metrics, vessel density (VD), perfusion density (PD) and area of intercapillary spaces (AIS) were obtained from superficial and deep capillary plexus (SCP, DCP). Only phenotype C identified by decreased  $VD \geq 2$  SD of healthy controls and phenotype B identified by subclinical macular edema with decreased  $VD < 2$  SD of healthy controls were included.

**Results:** One hundred twenty-two eyes from T2D individuals were included in study; 65 eyes (53%) were classified as phenotype B and 57 eyes (47%) as phenotype C. For phenotype B, progression was associated with thinning of the GCL + IPL (ETDRS 35, 1 year  $p = 0.013$ , 2 year

---

I. P. Marques · M. L. Ribeiro · T. P. Santos ·  
L. G. Mendes · D. Reste-Ferreira · A. R. Santos ·  
C. L. Lobo · J. G. Cunha-Vaz (✉)  
AIBILI-Association for Innovation and Biomedical  
Research on Light and Image, Azinhaga Sta. Comba,  
Celas, 3000-548 Coimbra, Portugal  
e-mail: cunhavaz@aibili.pt

I. P. Marques · M. L. Ribeiro · A. R. Santos ·  
C. L. Lobo · J. G. Cunha-Vaz  
Coimbra Institute for Clinical and Biomedical  
Research (iCIBR), Faculty of Medicine, University of  
Coimbra, Coimbra, Portugal

I. P. Marques · M. L. Ribeiro · A. R. Santos ·  
C. L. Lobo · J. G. Cunha-Vaz  
Center for Innovative Biomedicine and  
Biotechnology (CIBB), University of Coimbra, 3000-  
548 Coimbra, Portugal

A. R. Santos  
Department of Orthoptics, School of Health,  
Polytechnic of Porto, Porto, Portugal

C. L. Lobo  
Department of Ophthalmology, Centro Hospitalar e  
Universitário de Coimbra (CHUC), Coimbra,  
Portugal

I. P. Marques · A. R. Santos · C. L. Lobo  
Coimbra Ophthalmology Reading Centre (CORC),  
Coimbra, Portugal

$p < 0.001$ ; ETDRS 43–47, 2 year  $p = 0.003$ ) and vessel closure involving mainly the DCP for both ETDRS grades (ETDRS 35, 1 year  $p = 0.025$ , 2 year  $p = 0.034$ ; ETDRS 43–47, 1 year  $p = 0.011$ ). For phenotype C there was also progressive thinning of the GCL + IPL (ETDRS 35, in both years  $p \leq 0.001$ ; ETDRS 43–47, 1 year  $p = 0.002$ , 2 year  $p = 0.001$ ), with vessel closure involving mainly SCP (ETDRS 35, 1 year  $p = 0.012$ , 2 year  $p = 0.023$  in full-retina), which appeared to stabilize at maximal values in ETDRS grade 43–47 at the end of 2 years. ETDRS severity changes at the end of the 2-year period showed that worsening was associated with phenotype C with changes involving predominantly the SCP (VD,  $p = 0.005$ ; PD,  $p = 0.008$ ; AIS,  $p = 0.005$ ).

**Conclusions:** Association between ETDRS classification of NPDR severity and identification of different risk phenotypes offers new perspective to predict disease progression in T2D individuals with NPDR.

**Keywords:** Diabetes; Retinopathy; Capillary closure; Neurodegeneration

### Key Summary Points

#### *Why carry out this study?*

Unmet need: identification of eyes of individuals with nonproliferative diabetic retinopathy (NPDR) and T2D under acceptable metabolic control that are at risk for DR progression.

The aim of the study was to characterize disease progression in a 2-year period in eyes with mild and moderate NPDR comparing different phenotypes identified by the predominance of two major disease pathways: edema and ischemia.

#### *What was learned from the study?*

Both risk phenotypes, B and C, showed progression in retinal neurodegeneration, but different involvement of the retinal capillary circulation. Phenotype B disease progression occurs mainly through changes in the deep retinal capillary plexus whereas phenotype C progress mainly through changes in the superficial retinal capillary plexus.

The baseline characterization of DR phenotype in T2D individuals is an indicator of DR progression, and the study shows that in a 2-year period, individuals identified as phenotype C are associated with worsening of their retinopathy severity.

## INTRODUCTION

Diabetic retinopathy (DR) is a frequent complication of diabetes that may lead to loss of vision. Diabetes is now regarded as a global epidemic. It is estimated that by 2045 there will be 629 million people worldwide with diabetes. Considering that a third of people with diabetes develop signs of retinopathy with 10% developing some degree of vision loss, DR is a leading cause of blindness [1, 2].

Nonproliferative DR (NPDR) progresses silently from mild to moderate stages. However, its progression to more advanced stages, proliferative retinopathy and macular edema with vision loss varies from individual to individual. The cumulative occurrence of rates of progression from mild and moderate retinopathy to vision-threatening complications has been determined to be 14–16% [3, 4]. Therefore, predicting which people with mild to moderate NPDR are at risk of progression is of major relevance.

The activity of retinal disease and its progression varies from patient to patient, making identification of biomarkers of risk for progression of DR of great value. It is of particular note that changes in the retina can regress indicating

that there is also a real opportunity for drugs or other treatments to stop retinal disease progression [5]. Considering that treatments directed at the initial stages of NPDR, particularly treatments that can be administered outside of a clinical setting, such as oral or topical formulations, are particularly desirable, identification of risk profiles for progression of NPDR is a major goal.

Different phenotypes of NPDR progression have been previously identified by our group, as A, B and C, based on the predominance of different disease pathways. Phenotype A showed only neurodegenerative changes, whereas phenotype B was characterized by the presence of edema and phenotype C by the predominance of microvascular changes. Over a 5-year period only phenotype B and C developed vision-threatening complications [6–8].

This study is a 2-year analysis of the progression of a cohort of individuals with type 2 diabetes (T2D) with mild and moderate NPDR. We have previously published the results of the 1-year follow-up, and in our initial characterization of phenotypes, the presence of microvascular changes was identified by increased microaneurysm turnover (MAT) detected by a specific algorithm, the Retmarker [9]. However, to facilitate comparison of our results by other groups, considering that MAT is not widely used, and to translate the information into general clinical practice, in this 2-year analysis we decided to replace MAT metrics with definite microvascular nonperfusion in the retinal superficial capillary plexus ( $VD \leq 2$  SD of healthy controls) to identify the presence of microvascular changes and ischemia in phenotype C. Now, we are reporting on the results of the full 2-year study focusing on progression of microvascular changes considering Early Treatment Diabetic Retinopathy Study (ETDRS) grades and two different risk phenotypes, ischemia (phenotype C) and subclinical macular edema with minimal ischemia (phenotype B).

## METHODS

We are reporting here the results of the CORDIS 2-year prospective longitudinal observational

cohort study (ClinicalTrials.gov Identifier Number NCT03696810) in individuals with T2D with NPDR (levels 20, 35, 43 and 47 of the ETDRS severity scale) at demographic, systemic and ophthalmological levels. The 1-year progression data were the subject of a previous report [9]. The tenets of the Declaration of Helsinki were followed, and the study was reviewed and approved by the Association for Innovation and Biomedical Research on Light and Image (AIBILI) Ethics Committee for Health with the number CEC/194/18 (CORDIS). Written informed consent was signed by each participant, agreeing to participate in the study, after all procedures had been explained.

Individuals were included according to specified inclusion criteria, being classified as phenotype B or C, and followed for 2 years with three annual visits: baseline (0), 12 month (1 year) and 24 month (2 year). The study exclusion criteria comprised the presence of cataract or other disease that might interfere with fundus examinations, glaucoma, any eye surgery within a 6-month period before the baseline visit, other retinal vascular disease, any previous laser treatment or intravitreal injections, or dilation of pupil  $< 5$  mm.

After inclusion/exclusion criteria and new characterization of phenotypes, 122 eyes from individuals with T2D who had completed 2-year follow-up were considered for data analysis. There were 93 men (76%) and 29 women (24%) with diagnosed adult-onset T2D, aged 47–79 years. An age-matched healthy control population of 65 individuals was used as reference for demographic and ocular characteristics.

For each participant, demographics and systemic characteristics were collected by an experienced nurse at baseline visit, including age, duration of diabetes, co-morbidities, concomitant medication, physical and biometric measures (body weight and height), blood pressure evaluation and blood analyses to assess metabolic control, included plasma concentrations of hemoglobin A1c (HbA1c) and lipid fractionation identifying total cholesterol, high-density lipoprotein (HDL), low-density lipoprotein (LDL) and triglycerides. Exclusion criteria also included glycated HbA1c level  $>$

10% (85.8 mmol/mol) and any other systemic disease that could affect the eye, with special attention to uncontrolled systemic hypertension and history of heart disease.

Participants underwent a complete ophthalmology examination, which included best corrected visual acuity (BCVA), slit-lamp examination, color fundus photography (CFP), optical coherence tomography (OCT) and optical coherence tomography angiography (OCTA).

During the period of the study and outside of the study visits, participants were followed in our institution in accordance with the usual clinical practice.

Baseline characteristics of the study population are presented in Tables 1 and 2.

### Best Corrected Visual Acuity Evaluation

Best corrected visual acuity (BCVA) was evaluated and recorded as letters read at 4 m on ETDRS charts. Final BCVA letter score was calculated by adding the number of letters read at 4 m plus 30 (or the number of letters read at 1 m). BCVA was assessed using the Snellen scale and converted into logarithm units of the minimal angle of resolution (logMAR). The presence of any visual loss was recorded.

### Color Fundus Photography and ETDRS

Early Treatment Diabetic Retinopathy Study (ETDRS) classification was performed based on 7-field CFP images obtained at 30°/35° using a Topcon TRC 50DX camera (Topcon Medical Systems, Tokyo, Japan) with a resolution of 3596 × 2448 pixels. ETDRS grading scale and the DR severity score were classified at Coimbra Ophthalmology Reading Center (CORC), using a modified Airlie House classification scheme according to the ETDRS protocol. Classification was performed by two graders, with an inter-grader agreement of 93.7% [10].

### Optical Coherence Tomography (OCT) and OCT-Angiography

Central retinal thickness (CRT) and ganglion cell layer + inner plexiform layer (GCL + IPL) thickness at the inner ring were measured on each participant at each visit using the Macular Cube 512 × 128 (128 B-scans with 512 A-scans each) acquisition protocol available on the Cirrus Zeiss 5000 AngioPlex (Carl Zeiss Meditec, Dublin, CA, USA). Decreases (thinning) in GCL + IPL were considered to identify neurodegeneration.

OCTA vascular metrics were acquired in the central macular area using the angiography 3 × 3 mm acquisition protocol. This acquisition protocol consists of a set of 245 clusters of 4 B-scans repetitions, where each B-scan consists of 245 A-scans. The Carl Zeiss Meditec Density Exerciser (version: 10.0.12787; Carl Zeiss Meditec, Inc., Dublin, CA, USA) was used to calculate the perfusion density (PD), vessel density (VD) and foveal avascular zone (FAZ), detected at the superficial capillary plexus (SCP), deep capillary plexus (DCP) and full retina (FR). The area of intercapillary spaces (AIS) was calculated using the method previously described by our group [11]. Morphological operations that include the bottom-hat transform were applied to the binary slab of the en-face slabs generated by the Carl Zeiss Meditec Density Exerciser. AIS was computed for the SCP, DCP and FR. Quality check and normalization of signal strength were accomplished in all OCTA examinations as previously described [12].

### Characterization of Diabetic Retinopathy Phenotypes

Classification of DR phenotypes for each participant was performed using the values of VD in the SCP and CRT according to the following rules: phenotype C was identified by decreased values of VD of SCP  $\geq 2$  SD of a reference healthy population, and phenotype B was characterized by increased values of CRT ( $\geq 260$   $\mu\text{m}$  in women and  $\geq 275$   $\mu\text{m}$  in men) and with no decreased VD of SCP values  $\geq 2$  SD of a reference healthy population. CRT

**Table 1** Demographic, systemic and ocular characteristics at baseline (V1-0 months) by ETDRS severity group, comparison with healthy controls and comparison between the different ETDRS severity groups

	Healthy (N = 65)	ETDRS 20 (N = 12)	p value <sup>a</sup> (20 vs. healthy)	ETDRS 35 (N = 74)	p value <sup>a</sup> (35 vs. healthy)	ETDRS 43–47 (N = 36)	p value <sup>a</sup> (43–47 vs. healthy)	p value <sup>b</sup> (ETDRS severity groups)
<b>Demographic characteristics</b>								
Gender, male/ female N (%)	35/30 (53.8%/ 46.2%)	8/4 (66.7%/ 33.3%)		54/20 (73.0%/ 27.0%)		31/5 (86.1%/ 13.9%)		
Age (years), mean ± SD	67.26 ± 2.72	68.00 ± 4.69		67.07 ± 6.76		66.94 ± 7.14		
Diabetes duration (years), mean ± SD		19.33 ± 9.06		19.31 ± 7.41		20.31 ± 6.94		
<b>Systemic characteristics, mean ± SD</b>								
Body mass index (kg/m <sup>2</sup> )		26.66 ± 2.3		29.3 ± 3.95		30.14 ± 4.44		<b>0.032</b>
HbA1c (%)		6.88 ± 1.04		7.68 ± 1.19		8.01 ± 1.76		0.067
Total cholesterol (mg/dl)		168.42 ± 30.3		160.26 ± 41.81		162.22 ± 45.76		0.543
LDL cholesterol (mg/dl)		91.17 ± 24.81		90.32 ± 33.89		90.83 ± 34.44		0.858
HDL cholesterol (mg/dl)		48.17 ± 10.54		45.69 ± 11.77		43.67 ± 11.36		0.450
Triglycerides (mg/ dl)		144.83 ± 75.09		121.47 ± 58.85		138.61 ± 67		0.320
Systolic blood pressure (mmHg)		136.33 ± 14.54		139.15 ± 11.37		139.33 ± 11.59		0.829
Diastolic blood pressure (mmHg)		76.33 ± 3.87		72.49 ± 9.72		72.33 ± 6.89		0.236

Table 1 continued

Healthy (N = 65)	ETDRS 20 (N = 12)	p value <sup>a</sup> (20 vs. healthy)	ETDRS 35 (N = 74)	p value <sup>a</sup> (35 vs. healthy)	ETDRS 43–47 (N = 36)	p value <sup>a</sup> (43–47 vs. healthy)	p value <sup>b</sup> (ETDRS severity groups)
Ocular characteristics, mean ± SD							
BCVA (logMAR)	-0.03 ± 0.06		0.02 ± 0.09		0.01 ± 0.08		0.154
CRT (µm)	260.57 ± 18.30	< <b>0.001</b>	278.55 ± 19.96	< <b>0.001</b>	275.08 ± 20.99	<b>0.001</b>	0.586
GCL + IPL thickness (µm)	82.67 ± 5.46	0.862	79.89 ± 7.86	<b>0.042</b>	79.57 ± 6.74	<b>0.035</b>	0.267
FAZ circularity	0.65 ± 0.06	0.607	0.58 ± 0.11	< <b>0.001</b>	0.61 ± 0.11	<b>0.041</b>	0.136
FAZ area (mm <sup>2</sup> )	0.24 ± 0.10	0.094	0.23 ± 0.08	0.592	0.28 ± 0.11	0.132	<b>0.014</b>
Vessel density-IR- SCP (mm <sup>-1</sup> )	22.35 ± 0.87	<b>0.001</b>	20.54 ± 1.38	< <b>0.001</b>	20.56 ± 1.25	< <b>0.001</b>	0.194
Vessel density-IR- DCP (mm <sup>-1</sup> )	17.26 ± 2.16	0.096	15.86 ± 2.27	<b>0.001</b>	15.68 ± 1.94	< <b>0.001</b>	0.854
Vessel density-IR- FR (mm <sup>-1</sup> )	23.75 ± 0.9	<b>0.009</b>	22.29 ± 1.29	< <b>0.001</b>	22.27 ± 1.26	< <b>0.001</b>	0.325
Perfusion density- IR-SCP	0.4 ± 0.02	<b>0.029</b>	0.39 ± 0.02	< <b>0.001</b>	0.39 ± 0.02	<b>0.030</b>	0.634
Perfusion density- IR-DCP	0.33 ± 0.04	0.093	0.31 ± 0.04	<b>0.002</b>	0.31 ± 0.03	<b>0.006</b>	0.999
Perfusion density- IR-FR	0.42 ± 0.02	0.084	0.41 ± 0.02	<b>0.012</b>	0.42 ± 0.02	0.277	0.611
AIS-SCP (× 1000)	11.60 ± 3.18	< <b>0.001</b>	28.42 ± 11.02	< <b>0.001</b>	31.62 ± 10.62	< <b>0.001</b>	<b>0.015</b>
AIS-DCP (× 1000)	27.80 ± 8.95	<b>0.003</b>	41.74 ± 12.81	< <b>0.001</b>	48.13 ± 17.67	< <b>0.001</b>	0.171

**Table 1** continued

Healthy (N = 65)	ETDRS 20 (N = 12)	<i>p</i> value <sup>a</sup> (20 vs. healthy)	ETDRS 35 (N = 74)	<i>p</i> value <sup>a</sup> (35 vs. healthy)	ETDRS 43–47 (N = 36)	<i>p</i> value <sup>a</sup> (43–47 vs. healthy)	<i>p</i> value <sup>b</sup> (ETDRS severity groups)
AIS-FR (× 1000)	7.52 ± 2.62	<b>&lt; 0.001</b>	18.00 ± 7.87	<b>&lt; 0.001</b>	20.59 ± 8.26	<b>&lt; 0.001</b>	0.067

Bold values represent statistically significant alterations with *p* < 0.05

*N* number of participants, *SD* standard deviation, *ETDRS* Early Treatment Diabetic Retinopathy Study, *HbA1c* glycated hemoglobin, *LDL* low-density lipoprotein, *HDL* high-density lipoprotein, *BCVA* best corrected visual acuity, *CRT* central retinal thickness, *GCL* + *IPL* ganglion cell layer + inner plexiform layer, *FAZ* foveal avascular zone, *IR* inner ring, *SCP* superior capillary plexus, *DCP* deep capillary plexus, *FR* full retina, *AIS* area of intercapillary space

<sup>a</sup>Mann-Whitney *U*

<sup>b</sup>Kruskal-Wallis tests

reference values presented in this study are the reference for Zeiss Cirrus 5000 SD-OCT for subclinical macular edema [13, 14]. As mentioned above, only individuals classified with phenotype B or C were included in the study.

### Statistical Analysis

Data on each eye/patient are represented as means and corresponding standard deviations for continuous variables and absolute and relative frequencies for categorical and ordinal variables. The comparisons of baseline ocular characteristics between participants of each ETDRS severity group (ETDRS 20, ETDRS 35 and ETDRS 43–47) and healthy controls were performed with the Mann-Whitney *U* test. The Kruskal-Wallis test and all-pairwise post hoc comparisons with Bonferroni correction were used to compare systemic and ocular parameters among participants with different ETDRS levels (20, 35 and 43–47) and to compare characteristics between different diabetic retinopathy phenotypes and healthy controls. Changes in ocular characteristics at 1- and 2-year follow-up were assessed with the Wilcoxon signed rank test. A linear mixed model, using restricted maximum likelihood approach, was applied to study longitudinal changes, where visit (baseline, 12-month, and 24-month) was used as a continuous fixed variable and the ocular metrics, age, gender, diabetes durations and HbA1c were inserted as fixed covariables. The participants were used as a random variable (intercept only). The model was repeated as an additional fixed variable, the different phenotypes (B and C). To verify the linear mixed models' assumptions, homoscedasticity and normality of residuals in the models were visually inspected with residuals vs. predicted and Q-Q plots, respectively.

Data normality was assessed with the Shapiro-Wilk test. All statistical analyses were performed with Stata 16.1 (StataCorp LLC, College Station, TX, USA), and *p* values < 0.05 were considered statistically significant.

**Table 2** Comparison of baseline demographic, systemic and ocular characteristics between different diabetic retinopathy phenotypes and healthy controls

	Healthy ( <i>N</i> = 65)	Phenotype B ( <i>N</i> = 65)	Phenotype C ( <i>N</i> = 57)	<i>p</i> value
Demographic characteristics				
Gender, male/female <i>N</i> (%)	35/30 (53.8%/46.2%)	52/13 (80.0%/20.0%)	41/16 (71.9%/28.1%)	<b>0.005<sup>a</sup></b>
Age (years), mean ± SD	67.26 ± 2.72	67.57 ± 6.53	66.61 ± 6.84	0.410 <sup>b</sup>
Diabetes duration (years), mean ± SD		19.75 ± 8.15	19.44 ± 6.51	0.908 <sup>c</sup>
ETDRS levels				
ETDRS level 20		9 (13.8%)	3 (5.3%)	
ETDRS level 35		40 (61.5%)	34 (59.6%)	0.181 <sup>a</sup>
ETDRS level 43–47		16 (24.6%)	20 (35.1%)	
ETDRS changes				
Improved		16 (25%)	8 (14%)	0.312 <sup>a</sup>
Maintained		41 (63%)	40 (70%)	
Worsened		8 (12%)	9 (16%)	
Systemic characteristics, mean ± SD				
Body mass index (kg/m <sup>2</sup> )		28.59 ± 3.97	30.08 ± 4.05	<b>0.010<sup>c</sup></b>
HbA1c (%)		7.55 ± 1.16	7.86 ± 1.62	0.363 <sup>c</sup>
Total cholesterol (mg/dl)		162.6 ± 43.74	160.54 ± 39.9	0.972 <sup>c</sup>
LDL cholesterol (mg/dl)		89.98 ± 34.4	91.21 ± 31.72	0.612 <sup>c</sup>
HDL cholesterol (mg/dl)		47.08 ± 10.17	43.35 ± 12.68	<b>0.023<sup>c</sup></b>
Triglycerides (mg/dl)		127.71 ± 62.52	130.11 ± 64.38	0.873 <sup>c</sup>
Systolic blood pressure (mmHg)		139.8 ± 12.69	137.93 ± 10.46	0.120 <sup>c</sup>
Diastolic blood pressure (mmHg)		74.12 ± 8.73	71.33 ± 8.21	0.090 <sup>c</sup>
Ocular characteristics, mean ± SD				
BCVA (logMAR)		0.00 ± 0.08	0.03 ± 0.09	0.217 <sup>c</sup>
CRT (μm)	260.6 ± 18.3	285.6 ± 13.1	268.8 ± 21.8	< <b>0.001<sup>b</sup></b>
GCL + IPL thickness (μm)	82.7 ± 5.5	81.4 ± 6.9	78.7 ± 7.7	<b>0.017<sup>b</sup></b>
FAZ circularity	0.65 ± 0.06	0.60 ± 0.1	0.58 ± 0.11	< <b>0.001<sup>b</sup></b>
FAZ area (mm <sup>2</sup> )	0.24 ± 0.10	0.22 ± 0.1	0.25 ± 0.09	0.110 <sup>b</sup>
Vessel density-IR-SCP (mm <sup>-1</sup> )	22.35 ± 0.87	21.63 ± 0.71	19.6 ± 0.94	< <b>0.001<sup>b</sup></b>
Vessel density-IR-DCP (mm <sup>-1</sup> )	17.26 ± 2.16	16.78 ± 1.60	14.82 ± 2.22	< <b>0.001<sup>b</sup></b>
Vessel density-IR-FR (mm <sup>-1</sup> )	23.75 ± 0.9	23.25 ± 0.73	21.43 ± 0.97	< <b>0.001<sup>b</sup></b>



**Table 2** continued

	Healthy ( <i>N</i> = 65)	Phenotype B ( <i>N</i> = 65)	Phenotype C ( <i>N</i> = 57)	<i>p</i> value
Perfusion density-IR-SCP	0.40 ± 0.02	0.40 ± 0.02	0.38 ± 0.02	< <b>0.001</b> <sup>b</sup>
Perfusion density-IR-DCP	0.33 ± 0.04	0.32 ± 0.03	0.29 ± 0.04	< <b>0.001</b> <sup>b</sup>
Perfusion density-IR-FR	0.42 ± 0.02	0.43 ± 0.02	0.40 ± 0.02	< <b>0.001</b> <sup>b</sup>
AIS-SCP (× 1000)	3.71 ± 1.86	23.02 ± 10.06	34.35 ± 8.61	< <b>0.001</b> <sup>b</sup>
AIS-DCP (× 1000)	16.57 ± 6.45	39.25 ± 14.11	48.43 ± 14.36	< <b>0.001</b> <sup>b</sup>
AIS-FR (× 1000)	2.37 ± 1.36	15.01 ± 7.56	21.86 ± 6.91	< <b>0.001</b> <sup>b</sup>

Bold values represent statistically significant alterations with  $p < 0.05$

*N* number of participants, *SD* standard deviation, *ETDRS* Early Treatment Diabetic Retinopathy Study, *HbA1c* glycated hemoglobin, *LDL* low-density lipoprotein, *HDL* high-density lipoprotein, *BCVA* best corrected visual acuity, *CRT* central retinal thickness, *GCL + IPL* ganglion cell layer + inner plexiform layer, *FAZ* foveal avascular zone, *IR* inner ring, *SCP* superior capillary plexus, *DCP* deep capillary plexus, *FR* full retina, *AIS* area of intercapillary space

<sup>a</sup>Chi-square test results for categorical variables

<sup>b</sup>Kruskal-Wallis test and all-pairwise post hoc comparisons with Bonferroni correction for analysis between different DR phenotypes and healthy controls

<sup>c</sup>Mann-Whitney *U* test for systemic characteristics between phenotypes

## RESULTS

Of the 122 eyes analyzed, 12 (10%) were graded as ETDRS level 20 at baseline, 74 (61%) as ETDRS 35 and 36 (29%) as ETDRS 43–47. Demographic and baseline systemic and ocular parameters of these eyes are presented in Table 1 and compared with ocular parameters of 65 age-matched healthy control eyes.

Of the systemic variables only body mass index showed statistically significant differences between the different DR severity groups ( $p = 0.032$ ). Regarding the ocular parameters, increased thinning of the GCL + IPL, indicating neurodegenerative changes, was present in ETDRS grades 35 and 43–47 but not in grade 20 when compared to healthy controls. Furthermore, variable CRT is increased in all ETDRS grades when compared to healthy controls ( $p \leq 0.001$ ). FAZ area changes did not appear to reach significant levels when comparing to the healthy population but separated the three ETDRS grades included well ( $p = 0.014$ ). Pairwise comparisons indicated that the significant difference was set between those with ETDRS 20

and ETDRS 43–47 ( $p = 0.010$ ). The only other variable that separated the three ETDRS grades well was the changes in the AIS in the SCP ( $p = 0.015$ ) and the pairwise comparisons indicating in this variable that ETDRS 20 presented statistically lower than other ETDRS levels (ETDRS 35  $p = 0.043$  and ETDRS 43–47 = 0.006).

Microvascular OCTA metrics such as skeletonized VD, PD and AIS showed highly significant differences in all ETDRS grades when compared to age-matched healthy controls.

Table 2 shows baseline characteristics of the individuals classified with different DR phenotypes and healthy controls. Phenotype C presents higher values of body mass index ( $p = 0.010$ ) and lower values of HDL cholesterol ( $p = 0.023$ ) when compared to phenotype B.

Progression over the 1- and 2-year periods of follow-up, considering both ETDRS grades and both phenotypes, also showed clear differences in microvascular disease and neurodegenerative changes (Table 3). In eyes with mild NPDR (ETDRS grade 35) and classified as phenotype B, the microvascular changes occurred preferentially in the DCP in the first year of follow-up. For the second year the microvascular changes

**Table 3** One- and 2-year progression for each phenotype according to ETDRS severity groups

	Phenotype B				Phenotype C				
	Baseline (V0-0M)	1 year (V1-12M)	2 year (V2-24M)	p value (V0 vs. V1)	Baseline (V0-0M)	1 year (V1-12M)	2 year (V2-24M)	p value (V0 vs. V1)	p value (V0 vs. V2)
				V2)				V1)	V2)
ETDRS 35									
BCVA (logMAR)	0.01 ± 0.08	0.04 ± 0.09	0.05 ± 0.12	<b>0.013</b>	0.04 ± 0.10	0.05 ± 0.09	0.03 ± 0.1	0.732	0.950
CRT (µm)	286.75 ± 13.45	290.5 ± 26.01	293.65 ± 30.87	0.808	268.91 ± 22.14	267.18 ± 19.28	267.44 ± 22.89	0.682	0.331
GCL + IPL thickness (µm)	81.53 ± 6.94	81.21 ± 7.01	80.24 ± 6.91	<b>0.013</b>	77.97 ± 8.53	77.03 ± 8.56	76.79 ± 8.63	<b>0.001</b>	< <b>0.001</b>
FAZ circularity	0.60 ± 0.09	0.62 ± 0.08	0.61 ± 0.09	0.696	0.56 ± 0.11	0.57 ± 0.08	0.6 ± 0.08	0.634	0.074
FAZ area (mm <sup>2</sup> )	0.22 ± 0.08	0.22 ± 0.08	0.22 ± 0.08	0.455	0.24 ± 0.08	0.23 ± 0.09	0.25 ± 0.1	0.812	0.491
Vessel density-IR-SCP	21.57 ± 0.75	21.44 ± 0.99	21.16 ± 1.32	0.504	19.51 ± 1.07	20.02 ± 1.42	19.85 ± 1.3	0.067	<b>0.032</b>
Vessel density-IR-DCP	17.00 ± 1.56	16.07 ± 2.18	16.3 ± 1.94	<b>0.025</b>	14.71 ± 2.31	14.65 ± 2.31	14.64 ± 2.41	0.543	0.905
Vessel density-IR-FR	23.20 ± 0.76	23.18 ± 0.95	22.9 ± 1.16	0.992	21.38 ± 1.05	21.94 ± 1.36	21.8 ± 1.3	<b>0.012</b>	<b>0.023</b>
Perfusion density-IR-SCP	0.40 ± 0.02	0.40 ± 0.02	0.39 ± 0.03	0.053	0.37 ± 0.02	0.38 ± 0.02	0.37 ± 0.02	0.887	0.874
Perfusion density-IR-DCP	0.33 ± 0.03	0.31 ± 0.04	0.32 ± 0.03	<b>0.027</b>	0.29 ± 0.04	0.29 ± 0.04	0.29 ± 0.04	0.839	0.803
Perfusion density-IR-FR	0.43 ± 0.02	0.42 ± 0.02	0.42 ± 0.02	0.189	0.40 ± 0.02	0.4 ± 0.02	0.4 ± 0.02	0.919	0.944
ETDRS 43–47									
AIS-SCP (× 1000)	22.60 ± 10.12	23.95 ± 9.15	24.99 ± 11.83	0.163	34.24 ± 8.63	34.00 ± 11.85	34.54 ± 12.24	0.824	0.698
AIS-DCP (× 1000)	38.11 ± 13.45	45.28 ± 14.39	43.68 ± 19.67	<b>0.021</b>	45.38 ± 11.17	44.44 ± 10.59	47.93 ± 18.99	0.761	0.738
AIS-FR (× 1000)	14.598 ± 7.60	15.22 ± 7.30	15.97 ± 8.62	0.433	21.40 ± 6.63	22.14 ± 8.77	22.29 ± 9.52	0.968	0.986
ETDRS 43–47									
BCVA (logMAR)	0.02 ± 0.08	0.04 ± 0.12	0.04 ± 0.11	0.426	0.01 ± 0.08	0.02 ± 0.08	0.01 ± 0.10	0.399	0.933
CRT (µm)	285.63 ± 13.41	283.75 ± 16.07	285.00 ± 18.65	0.456	266.65 ± 22.39	272.5 ± 25.87	266.50 ± 17.91	0.435	0.891

**Table 3** continued

	Phenotype B				Phenotype C				
	Baseline (V0-0M)	1 year (V1-12M)	2 year (V2-24M)	<i>p</i> value (V0 vs. V1)	Baseline (V0-0M)	1 year (V1-12M)	2 year (V2-24M)	<i>p</i> value (V0 vs. V1)	<i>p</i> value (V0 vs. V2)
GCL + IPL thickness (µm)	79.27 ± 6.87	78.00 ± 7.36	77.13 ± 6.88	0.094	79.8 ± 6.8	78.37 ± 7.78	77.95 ± 7.52	<b>0.002</b>	<b>0.001</b>
FAZ circularity	0.60 ± 0.12	0.50 ± 0.13	0.61 ± 0.1	0.131	0.61 ± 0.10	0.56 ± 0.10	0.60 ± 0.08	0.058	0.117
FAZ area (mm <sup>2</sup> )	0.27 ± 0.14	0.26 ± 0.14	0.28 ± 0.12	0.322	0.28 ± 0.09	0.28 ± 0.09	0.28 ± 0.07	0.391	0.495
Vessel density-IR-SCP	21.75 ± 0.66	20.85 ± 1.14	21.17 ± 1.26	<b>0.002</b>	19.68 ± 0.74	19.72 ± 1.01	19.82 ± 1.08	0.623	0.701
Vessel density-IR-DCP	16.37 ± 1.46	14.07 ± 2.41	15.65 ± 1.59	<b>0.011</b>	15.16 ± 2.12	13.55 ± 2.47	14.47 ± 1.82	<b>0.018</b>	0.241
Vessel density-IR-FR	23.39 ± 0.64	22.52 ± 0.91	22.75 ± 1.01	<b>0.004</b>	21.43 ± 0.90	21.68 ± 1.05	21.79 ± 1.04	0.210	0.202
Perfusion density-IR-SCP	0.41 ± 0.01	0.39 ± 0.02	0.40 ± 0.03	<b>0.003</b>	0.38 ± 0.02	0.37 ± 0.02	0.37 ± 0.02	0.066	0.083
Perfusion density-IR-DCP	0.32 ± 0.03	0.28 ± 0.04	0.31 ± 0.03	<b>0.003</b>	0.30 ± 0.04	0.27 ± 0.04	0.29 ± 0.03	<b>0.023</b>	0.145
Perfusion density-IR-FR	0.43 ± 0.02	0.41 ± 0.01	0.42 ± 0.02	<b>0.009</b>	0.41 ± 0.02	0.40 ± 0.02	0.40 ± 0.02	0.182	0.165
AIS-SCP (× 1000)	25.70 ± 11.06	30.15 ± 14.49	29.97 ± 13.68	0.296	36.06 ± 7.95	38.38 ± 12.62	33.19 ± 9.83	0.490	0.143
AIS-DCP (× 1000)	40.78 ± 14.22	54.83 ± 29.58	45.84 ± 12.79	<b>0.017</b>	53.64 ± 18.31	53.65 ± 16.00	49.91 ± 10.57	0.922	0.756
AIS-FR (× 1000)	16.84 ± 8.03	20.57 ± 12.6	19.56 ± 9.86	0.268	23.41 ± 7.42	24.72 ± 11.69	20.39 ± 7.69	0.891	0.058

Bold values represent statistically significant alterations with *p* < 0.05 using the Wilcoxon sign test

*N* number of participants, *SD* standard deviation, *ETDRS* Early Treatment Diabetic Retinopathy Study, *HbA1c* glycated hemoglobin, *LDL* low-density lipoprotein, *HDL* high-density lipoprotein, *BCVA* best corrected visual acuity, *CRT* central retinal thickness, *GCL* + *IPL* ganglion cell layer + inner plexiform layer, *FAZ* foveal avascular zone, *IR* inner ring, *SCP* superior capillary plexus, *DCP* deep capillary plexus, *FR* full retina, *AIS* area of intercapillary space

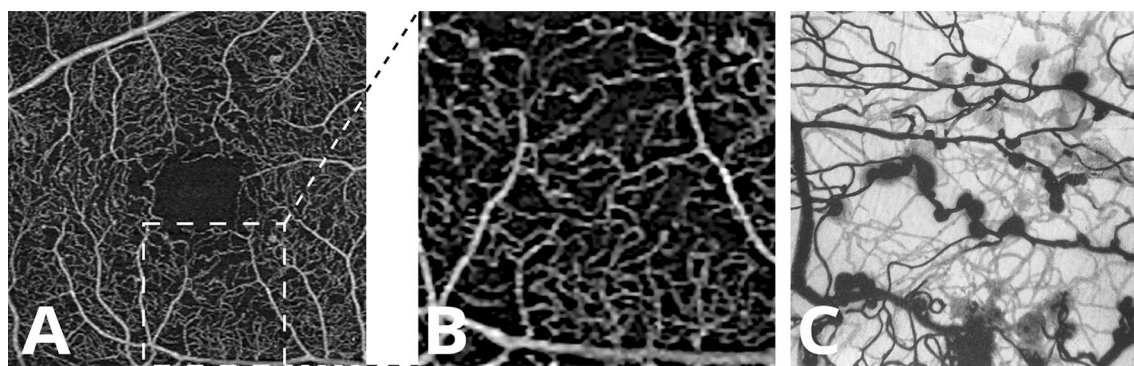


**Fig. 1** Example of capillary occlusion and preferential vessels (shunts) in diabetic eyes. **A** OCT angiography acquisition of the right eye of a phenotype C diabetic retinopathy patient with the highlighted area represented in **B**, capillary occlusion and enlarged preferential vessels.

**C** A post-mortem digested diabetic retina from a different individual injected with Indian ink showing similar vascular patterns characterized by capillary occlusion and enlarged preferential vessels

remained predominantly in the DCP but showed some degree of progression also in the SCP. In eyes with ETDRS grade 35 but with phenotype C, there is preferential involvement of the SCP, demonstrated by a decrease in skeletonized vessel density.

In the eyes with moderate NPDR (ETDRS grade 43–47), a more severe stage of NPDR and classified as phenotype B there is a decrease in vessel and perfusion densities in the superficial and deep retinal capillary plexus with stabilization in the 2nd year of follow-up. In phenotype C, there is also decrease in both vessel and perfusion densities involving predominantly the deep capillary plexus with later stabilization. In ETDRS grades 43 and 47, there is evidence of stabilization of the changes in VD, PD and AIS at the end of 2-year follow-up (Fig. 1).

When analyzing ETDRS severity changes at the 2-year follow-up (Table 4), 17 eyes (14%) showed worsening, whereas 24 eyes (20%) showed improvement. The eyes that showed retinopathy severity worsening were associated with phenotype C when compared with phenotype B and the differences were significant, involving predominantly the SCP (VD,  $p = 0.005$ ; PD,  $p = 0.008$ , AIS,  $p = 0.005$ ).

Multiple linear regression analysis was performed to evaluate the progression over the 2-year follow-up period, and our data showed significant differences across the time for several metrics; GCL + IPL thinning exhibited a

progression rate of  $-0.372 \mu\text{m}/\text{year}$  ( $p < 0.001$ ); vessel density involving predominantly the DCP showed a progression rate of  $-0.131 \text{mm}^{-1}/\text{year}$  ( $p = 0.039$ ), whereas perfusion density showed a progression rate of  $-0.002 \text{mm}^{-1}/\text{year}$  at SCP ( $p = 0.001$ ); DCP ( $p = 0.050$ ) and FR ( $p = 0.012$ ). Moreover, only the GCL + IPL thinning was negatively associated with age ( $-0.353 \mu\text{m}/\text{year}$ ,  $p \leq 0.001$ ) and with gender, with women showing less thinning of GCL + IPL than men ( $p = 0.001$ ).

The microvascular progression over 2 years in patients with phenotype B differed from phenotype C in skeletonized VD ( $2 \text{mm}^{-1}$ ,  $p \leq 0.001$ ), PD ( $0.03 \text{mm}^{-1}$ ,  $p \leq 0.001$ ) and AIS ( $-10 \times 1000/\text{year}$ ,  $p \leq 0.001$ ). Furthermore, only age was negatively associated ( $p \leq 0.001$ ).

## DISCUSSION

This study showed that the combination of OCT and OCTA examinations identifies the different stages of NPDR well, and this was demonstrated by the observations performed at baseline. The study also showed that different risk phenotypes for DR progression have different patterns of disease progression in mild and moderate NPDR, offering the opportunity for an improved characterization of NPDR regarding disease progression and establishment of risk profiles for DR progression.

**Table 4** Comparison of OCTA metrics at V4 (24 months) by phenotype, separated by DR severity step changes

	ETDRS step worsening			ETDRS step improvement		
	Phenotype B	Phenotype C	<i>p</i> value	Phenotype B	Phenotype C	<i>p</i> value
Vessel density-IR-SCP (mm <sup>-1</sup> )	22.55 ± 1.06	20.03 ± 1.22	<b>0.005</b>	21.14 ± 1.45	20.59 ± 0.77	0.267
Vessel density-IR-DCP (mm <sup>-1</sup> )	17.59 ± 1.19	15.27 ± 2.26	<b>0.029</b>	15.91 ± 2.09	15.27 ± 1.75	0.441
Vessel density-IR-FR (mm <sup>-1</sup> )	23.91 ± 1.28	22.02 ± 1.24	<b>0.036</b>	22.69 ± 1.34	22.44 ± 0.92	0.482
Perfusion density-IR-SCP	0.42 ± 0.02	0.38 ± 0.02	<b>0.008</b>	0.39 ± 0.03	0.38 ± 0.01	0.267
Perfusion density-IR-DCP	0.34 ± 0.03	0.30 ± 0.04	0.081	0.31 ± 0.04	0.30 ± 0.03	0.616
Perfusion density-IR-FR	0.44 ± 0.02	0.41 ± 0.02	0.066	0.41 ± 0.03	0.41 ± 0.01	0.616
AIS-SCP (× 1000)	20.03 ± 4.20	33.32 ± 10.90	<b>0.005</b>	26.22 ± 15.39	28.26 ± 8.29	0.267
AIS-DCP (× 1000)	42.58 ± 9.77	53.13 ± 30.14	0.456	40.36 ± 13.21	44.92 ± 10.47	0.570
AIS-FR (× 1000)	13.20 ± 4.85	21.16 ± 8.11	0.050	17.87 ± 10.97	17.97 ± 6.78	0.402

Bold values represent statistically significant alterations with  $p < 0.05$  using the Mann-Whitney  $U$  test

*ETDRS* Early Treatment Diabetic Retinopathy Study, *IR* inner ring, *SCP* superior capillary plexus, *DCP* deep capillary plexus, *FR* full retina, *AIS* area of intercapillary space

OCT and OCTA metrics offer important information on the changes occurring in DR. OCT allows the determination of the degree of neurodegenerative changes and of its progression and identifies changes in CRT, indicating the presence of absence of macular thickening. OCTA allows the quantification of microvascular changes by determining skeletonized VD and AIS, considered to be representative of vessel closure and PD, which may represent changes in blood flow. The information obtained from these variables on the three main disease pathways, neurodegeneration, edema and ischemia, which characterize the progression of DR [15], may allow improved grading of the severity of retinal disease and its progression offering an opportunity to identify risk profiles for DR progression. The characterization of phenotypes in this analysis was based on VD of the SCP obtained with OCTA. This choice was due to the generalized access to an OCTA device, the involvement of the retinal SCP since the early stages of NPDR [12] and the robustness of measurements performed on the SCP, which are obtained directly from the OCTA device.

Retinal vascular disease progression in NPDR showed different patterns in phenotypes B and C in mild (ETDRS grade 35) and moderate

(ETDRS grade 43–47) cases over the 1- and 2-year follow-up periods. Progression of mild and moderate NPDR (ETDRS grades 35 and 43–47) with phenotype B, characterized by the presence of subclinical macular edema and absence of definite ischemia, appears to occur mainly by microvascular changes occurring in the DCP, representing a milder form of NPDR. Progression of mild and moderate NPDR (ETDRS grades 35 and 43–47) with phenotype C, identified at baseline by the presence of advanced capillary closure in the SCP, appears to occur mainly through involvement of the SCP reaching maximal levels in the central retina after 2 years of follow-up, probably because of shifting of the progressive vascular closure to more peripheral regions of the retina, suggesting more rapid progression to a proliferative stage [16].

DR is a complex disease associated with a wide range of body alterations, and its progression has been shown to vary between different individuals. Our studies have proposed three major different phenotypes of progression, A, B and C, with distinct risks for disease severity progression and development of vision-threatening complications [7]. Other studies have shown that different groups of T2D individuals

have different courses for disease progression. It is important to realize also that it is necessary to consider not only progression but also regression of the disease [17]. Our study shows that in a 2-year period only 14% of the eyes with NPDR and ETDRS grade 20, 35 and 43–47 showed worsening characterized by at least one-step change in ETDRS severity grading whereas 20% showed improvement in ETDRS severity grading. It showed also that worsening of NPDR is associated with the presence of phenotype C, the ischemic phenotype. This finding has relevance when trying to identify risk for progression of mild and moderate DR. Identification of the risk phenotype and its presence at a specific stage of disease, characterized by the ETDRS severity grading, has the potential to establish a risk profile for a specific patient with potential value for the clinical management of diabetic retinal disease [18].

Our study confirms also that phenotype C, identified by the presence of advanced microvascular closure and ischemia, progresses through profound remodeling of the retinal capillary circulation, probably associated with the development of enlarged preferential vascular channels bypassing the areas of capillary closure [19, 20] (Fig. 1). This is apparently associated with progressive involvement of more peripheral regions of the retina and may explain the stabilization of the capillary closure identified by the OCTA metrics of VD and AIS in the central retina found in the 2nd year in this study. These findings reinforce the need for wide-field images using swept-source OCTA to characterize properly the extent of ischemia in moderate to severe NPDR [16].

We found also that variables that showed progression at 1 year could stabilize in the 2-year follow-up period. This observation confirms the complexity of diabetic retinal disease progression reinforcing the need to combine risk markers of progression such as ETDRS severity grading with phenotype characterization to establish risk profiles that may identify better disease progression in an individual patient.

The data obtained in this 2-year longitudinal study demonstrate the progression of microvascular closure in NPDR well. Initially,

the capillary closure occurs in the SCP (ETDRS grade 20, Table 1), with progression occurring mainly through vessel closure in the DCP (ETDRS grade 35, Table 3). Later, there is a progressive increase in vessel closure in the DCP until stabilization through development of preferential thoroughfare channels with increased involvement of the peripheral regions of retina.

In another two recent follow-up studies by our group in different patient cohorts, one performed during a 5-year period using OCT and another for a 3-year period using both OCT and OCTA, we verified that the risk of retinopathy progression, identified by ETDRS gradings, is different between different individuals with type 2 diabetes and that ocular imaging risk markers (CRT and GCL + IPL thickness) are stronger predictors of disease progression than systemic markers of metabolism control [6, 7].

The results reported here also confirm that the alterations occurring in the diabetic retina are reversible until relatively late in the disease process and vary between individuals [5, 6]. There is indeed marked variability with changes showing signs of regression at the 2-year examination compared with the 1-year examination, confirming reversibility of the ocular alterations identified by OCT and OCTA. The reversibility of the microvascular alterations opens the door for early interventions with the possibility of stopping or delaying disease progression.

A major limitation of this study is the focus on the initial stages of DR, including only eyes with ETDRS levels 20, 35 and 43–47 from individuals with T2D. These eyes are at a low risk of progression and development of vision-threatening complications. Another limitation is the lack of wide-field imaging, restricting our conclusions to observations registered in the central retina. The relatively small number of individuals included in the study and the rather restricting inclusion criteria, focusing on a relatively well-controlled population, are also a limitation of the study. However, this limitation offers an added value, which is the possibility of identifying risk profiles early in the

disease process and the development of timely management strategies.

## CONCLUSIONS

The results reported here offer promising perspectives for personalized management of DR. After diagnosis of NPDR and still in the initial stages of the disease, different phenotypes can be identified based on ocular imaging procedures, OCT and OCTA, which are non-invasive and easy to perform. These phenotypes show different patterns of disease progression. The association of phenotype characterization and severity staging of the retinopathy, establishing risk profiles of NPDR, has the potential to contribute to improved and timely management of DR.

## ACKNOWLEDGEMENTS

**Funding.** This work was supported by AIBILI, COMPETE Portugal2020, Foundation for Science and Technology (project no. 02/SAICT/2017-032412) and the Fundo de Inovação, Tecnologia e Economia Circular (FITEC)-Programa Interface (FITEC/CIT/2018/2). No funding or sponsorship was received for the publication of this article.

**Authorship.** All named authors meet the International Committee of Medical Journal Editors (ICMJE) criteria for authorship for this article, take responsibility for the integrity of the work as a whole, and have given their approval for this version to be published.

**Author Contributions.** Inês P. Marques, Maria L. Ribeiro, Torcato P. Santos, Luís G. Mendes, Débora Reste-Ferreira and Ana R. Santos collected data, analyzed, wrote and reviewed and edited the manuscript. Conceição L. Lobo and José Cunha-Vaz assisted in the analysis and interpretation of the data and wrote the manuscript. José Cunha-Vaz is the guarantor of this work and, as such, had full access to all the data in the study and takes responsibility for the

integrity of the data and the accuracy of the data analysis. All authors have read and agreed to the published version of the manuscript.

**Disclosures.** Inês P. Marques, Maria L. Ribeiro, Torcato P. Santos, Luís G. Mendes, Débora Reste-Ferreira, Ana R. Santos and Conceição L. Lobo declare no conflicts of interest. José Cunha-Vaz reports grants from Carl Zeiss Meditec and is a consultant for Alimera Sciences, Allergan, Bayer, Gene Signal, Novartis, Pfizer, Precision Ocular Ltd., Roche, Sanofi-Aventis, Vifor Pharma and Carl Zeiss Meditec. The funders had no role in the design or writing of the manuscript.

**Compliance with Ethics Guidelines.** The tenets of the Declaration of Helsinki were followed, and approval was obtained from the AIBILI Ethics Committee for Health with the number NCT03696810 (ClinicalTrials.gov identifier).

Written informed consent was obtained by each participant agreeing to participate in the study.

**Data Availability.** The datasets generated during and/or analyzed during the current study are available from the corresponding author on reasonable request.

**Open Access.** This article is licensed under a Creative Commons Attribution-NonCommercial 4.0 International License, which permits any non-commercial use, sharing, adaptation, distribution and reproduction in any medium or format, as long as you give appropriate credit to the original author(s) and the source, provide a link to the Creative Commons licence, and indicate if changes were made. The images or other third party material in this article are included in the article's Creative Commons licence, unless indicated otherwise in a credit line to the material. If material is not included in the article's Creative Commons licence and your intended use is not permitted by statutory regulation or exceeds the permitted use, you will need to obtain permission directly from the copyright holder. To view a copy of this licence,

visit <http://creativecommons.org/licenses/by-nc/4.0/>.

## REFERENCES

1. Cheung N, Mitchell P, Wong TY. Diabetic retinopathy. *Lancet* (London, England). 2010;376:124–36.
2. Narayan KMV, Boyle JP, Geiss LS, et al. Impact of recent increase in incidence on future diabetes burden: US, 2005–2050. *Diabetes Care*. 2006;29:2114–6.
3. Marques IP, Madeira MH, Messias AL, et al. Different retinopathy phenotypes in type 2 diabetes predict retinopathy progression. *Acta Diabetol*. 2021;58(2):197–205.
4. Sato Y, Lee Z, Hayashi Y. Subclassification of proliferative diabetic retinopathy and glycemic control: relationship between mean hemoglobin A1C value and development of proliferative diabetic retinopathy. *Jpn J Ophthalmol*. 2021;45:523–7.
5. Marques IP, Kubach S, Santos T, et al. Optical coherence tomography angiography metrics monitor severity progression of diabetic retinopathy—3-year longitudinal study. *J Clin Med*. 2021;10:2296.
6. Cunha-Vaz J, Ribeiro L, Lobo C. Phenotypes and biomarkers of diabetic retinopathy. *Prog Retin Eye Res*. 2014;41:90–111.
7. Marques IP, Madeira MH, Messias AL, et al. Retinopathy phenotypes in type 2 diabetes with different risks for macular edema and proliferative retinopathy. *J Clin Med*. 2020;9:1433.
8. Martinho AC-V, Marques IP, Messias AL, et al. Ocular and systemic risk markers for development of macular edema and proliferative retinopathy in type 2 diabetes: a 5-year longitudinal study. *Diabetes Care*. 2021;44:e12–4.
9. Ribeiro L, Marques IP, Coimbra R, et al. Characterization of one-year progression of risk phenotypes of diabetic retinopathy. *Ophthalmol Ther*. 2022;11(1):333–45.
10. Santos AR, Costa MÁ, Schwartz C, et al. Optical coherence tomography baseline predictors for initial best-corrected visual acuity response to intravitreal anti-vascular endothelial growth factor treatment in eyes with diabetic macular edema: the CHARTRES study. *Retina*. 2018;38:1110–9.
11. Mendes L, Marques IP, Cunha-Vaz J. Comparison of different metrics for the identification of vascular changes in diabetic retinopathy using OCTA. *Front Neurosci*. 2021;15: 755730.
12. Lei J, Durbin MK, Shi Y, et al. Repeatability and reproducibility of superficial macular retinal vessel density measurements using optical coherence tomography angiography en face images. *JAMA Ophthalmol*. 2017;135:1092.
13. Ribeiro L, Bandello F, Tejerina AN, et al. Characterization of retinal disease progression in a 1-year longitudinal study of eyes with mild nonproliferative retinopathy in diabetes type 2. *Investig Ophthalmol Vis Sci*. 2015;56:5698–705.
14. Bandello F, Tejerina AN, Vujosevic S, et al. Retinal layer location of increased retinal thickness in eyes with subclinical and clinical macular edema in diabetes type 2. *Ophthalmic Res*. 2015;54:112–7.
15. Marques IP, Alves D, Santos T, et al. Multimodal imaging of the initial stages of diabetic retinopathy: different disease pathways in different patients. *Diabetes*. 2019;68:648–53.
16. Santos T, Warren LH, Santos AR, et al. Swept-source OCTA quantification of capillary closure predicts ETDRS severity staging of NPDR. *Br J Ophthalmol*. 2022;106:712–8.
17. Zavrelova H, Hoekstra T, Alsema M, et al. Progression and regression: distinct developmental patterns of diabetic retinopathy in patients with type 2 diabetes treated in the diabetes care system west-friesland, the Netherlands. *Diabetes Care*. 2011;34:867–72.
18. Cunha-Vaz J, Mendes L. Characterization of risk profiles for diabetic retinopathy progression. *J Pers Med*. 2021;11:826.
19. Cogan DG, Kuwabara T. Capillary shunts in the pathogenesis of diabetic retinopathy. *Diabetes*. 1963;12:293–300.
20. Cunha-Vaz JG. Pathophysiology of diabetic retinopathy. *Br J Ophthalmol*. 1978;62:351–5.